



HAL
open science

A comprehensive synthetic database of global seismic losses covering the period 1967–2018

Cyrielle Dollet, Philippe Guéguen, Andres Hernandez

► **To cite this version:**

Cyrielle Dollet, Philippe Guéguen, Andres Hernandez. A comprehensive synthetic database of global seismic losses covering the period 1967–2018. *Bulletin of Earthquake Engineering*, 2023, 21 (9), pp.4265-4288. 10.1007/s10518-023-01695-x . hal-04320613

HAL Id: hal-04320613

<https://hal.science/hal-04320613>

Submitted on 4 Dec 2023

HAL is a multi-disciplinary open access archive for the deposit and dissemination of scientific research documents, whether they are published or not. The documents may come from teaching and research institutions in France or abroad, or from public or private research centers.

L'archive ouverte pluridisciplinaire **HAL**, est destinée au dépôt et à la diffusion de documents scientifiques de niveau recherche, publiés ou non, émanant des établissements d'enseignement et de recherche français ou étrangers, des laboratoires publics ou privés.

1 **A comprehensive synthetic database of global seismic losses**
2 **covering the period 1967-2018.**

3
4
5 Cyrielle Dollet¹, Philippe Guéguen¹, Andres Hernandez^{1,2}

6
7 ¹ISTerre, Université Grenoble Alpes, CNRS, IRD, Université Savoie Mont-Blanc, Université Gustave
8 Eiffel

9 ²Fugro, France

10
11
12
13
14
15
16 Bulletin of Earthquake Engineering volume 21, pages 4265–4288 (2023)
17 <https://doi.org/10.1007/s10518-023-01695-x>

18
19
20 **Corresponding author:**

21 Philippe Guéguen

22 ISTerre

23 Philippe.gueguen@univ-grenoble-alpes.fr

24
25
26
27
28
29

30 **Abstract**

31 This work aims to construct a synthetic database of human and economic seismic
32 losses. For weak-to-moderate magnitude and older earthquakes, the catalogs of
33 losses are incomplete, which limits the creation of probabilistic based loss models.
34 Furthermore, the number of earthquakes involving losses has increased in recent
35 years, following a non-stationary Poisson distribution with a rate proportional to the
36 exposed population and GDP. First, this study involved defining a series of empirical
37 models (from definition of magnitude to losses) tested by the likelihood method
38 applied to data from 377 earthquakes with variables related to exposure (exposed
39 population and exposed GDP) and consequences (economic losses, number of
40 fatalities and injuries). For these 377 earthquakes, the spatial variation of the hazard
41 was deduced from USGS ShakeMaps and the social and economic losses evaluated
42 were made stationary by taking into account exposure evolving over time. We then
43 built a synthetic database of seismic losses from the ISC-GEM catalog of epicenters,
44 which is assumed to be complete and homogeneous since 1967 for magnitudes > 5.
45 The combination of the 377 events and the synthetic data indicates that earthquakes
46 of magnitudes [5.5; 6.9] represent 36% of all economic losses, 56% of all fatalities,
47 and 71% of injuries. An occurrence model was then designed to predict the evolution
48 of losses over the next years.

49

50 **Keywords:** risk, losses, moderate earthquakes, database

51

52

53

1. Introduction

54

55 Major seismic catastrophes generate huge economic losses and are usually
56 associated with the most severe earthquakes (usually $M > 7$, Holzer and Savage,
57 2013). However, with the growing concentration of populations and economies in
58 increasingly dense urban areas, even moderate earthquakes (magnitude around 6)
59 can cause significant direct and indirect economic losses and a number of victims
60 that, although lower, remains unacceptable (e.g., Aquila/Italy, 2009, M 6.3, 309
61 victims, 0.1% GDP - Gross Domestic Product; Christchurch/New Zealand, 2011, M
62 6.3, 168 victims, 10% GDP; Emilia-Romana/Italy, 2012, M 6.1, 27 victims, 0.1%
63 GDP). To evaluate the risks represented by these seismic events globally or within a
64 specific region, we adapted a procedure used for probabilistic seismic hazard
65 analysis (PSHA) to determine the annual probability (or rate) of suffering losses.

66 Past events naturally provide key information for modeling what might happen in the
67 future. To perform a probabilistic risk analysis for a given region, a catalog of losses
68 associated with earthquakes must be as homogeneous as possible, covering the
69 longest possible time period (to have enough observations to extrapolate to the lower
70 rates of occurrence in which we are interested), and from the smallest magnitude (to
71 be as complete as possible). To avoid certain conventional biases that are also found
72 in PSHA, such as the fusion of catalogs of different origins or the conversion of basic
73 parameters (e.g., magnitude conversion), global catalogs are used to ensure the
74 homogeneity of the earthquake information and associated losses, and to reduce the
75 bias of the frequency-loss distributions. The complete ISC-GEM catalog (2019) for
76 global earthquakes of magnitudes 5 to 8 for the period 1967-2015 (Di Giacomo et al.,
77 2018) shows that moderate magnitudes (around 6) occur frequently. At the same
78 time, Nievas et al. (2020a; 2020b) showed that the information concerning moderate
79 earthquake losses is incomplete. Dollet and Guéguen (2022) made the same
80 observation by assessing the global occurrence models for human and economic
81 losses due to earthquakes from 1967 to 2018, considering the exposed GDP
82 (GDP_{Exp}) and population (POP_{Exp}) and by exploring the information in international
83 loss databases (e.g., EM-Dat, NOAA, etc.). These international databases list the

84 consequences of the most recent seismic events, but the magnitude of completeness
85 associated with the losses remains high (Nichols and Beaver, 2008; Holzer and
86 Savage, 2013; Dollet and Guéguen, 2022). Finally, although earthquake occurrence
87 follows a stationary Poisson distribution, seismic losses obey a non-stationary
88 distribution with a rate of occurrence proportional to the increase in population
89 (Holzer and Savage, 2013) and therefore the economic assets exposed.

90 Most loss estimation models are derived by regression from hazard-, exposure- and
91 consequences-related parameters (e.g. among others, Nichols and Beavers, 2003;
92 Jaiswal and Wald, 2010; Heatwole and Rose, 2013; Guettiche and al., 2017). For the
93 hazard, the ISC-GEM catalog (2019) provides earthquake magnitude and location.
94 However, unlike magnitude, macroseismic intensity (not recorded in ISC-GEM, 2019)
95 provides spatially variable parameter of hazard, to be crossed with a spatially
96 variable exposure (Jaiswal and Wald, 2010; 2013). Consequences depend on
97 exposure, such as exposed population and regional GDP or GDP per capita. These
98 two parameters are essential for predictions (e.g. among others, Christoskov and
99 Samardjieva, 1984; Cha, 1998; Badal and Samardjieva, 2002; Wyss and
100 Trendafilosky, 2011; Spence and al., 2011; Jaiswal and Wald, 2013; Heatwole and
101 Rose, 2013 ; Guettiche et al., 2017) and vary over time, making the process non-
102 stationary (Holzer and Savage, 2013). Dollet and Guéguen (2022) therefore compiled
103 a database (LEQ377) associating ShakeMaps and economic and human losses in
104 relation to the exposed population and exposed GDP at the time of the earthquake.
105 They also concluded on the incompleteness of the losses reported in the
106 international catalogs, in particular for low to moderate magnitude earthquakes,
107 essential to the definition of occurrence models.

108
109 The objective of this study is to build a complete and homogeneous catalog of
110 seismic losses for $M > 5$ earthquakes to assess annual occurrence rates. Using the
111 data available in the LEQ377 database (Dollet and Guéguen, 2022), we followed a
112 step-by-step procedure based on traditional practices used for performance-based
113 evaluation or seismic hazard probability i.e., by estimating macroseismic intensities
114 from magnitudes, then losses for a given exposure. Conversion or prediction models
115 were then derived from the observation data compiled by Dollet and Guéguen (2022)
116 for earthquakes of magnitudes 5-8 over the period 1967-2018 with epicentral

117 intensity larger than V , testing models efficiency at each step using the likelihood
118 method (Scherbaum et al., 2004). The models were then applied to the complete
119 ISC-GEM database (2019) for magnitudes >5 for the period 1967-2018 (Di Giacomo
120 et al., 2018) to get a synthetic catalogue of losses. Finally, annual probabilities (or
121 occurrence rate models) for human and economic losses are discussed.

122

123 **2. Data**

124

125 The data used here to develop the seismic loss models were taken from the LEQ445
126 database (Dollet and Guéguen, 2022). This database includes seismic events having
127 on the one hand, a spatial representation of the macroseismic intensity in the form of
128 Shakemap and, on the other hand, causing social or economic losses recorded over
129 the period 1967-2018.

130

131 Hazard-related data were taken from the Atlas of ShakeMaps (Wald et al., 1999;
132 Allen et al., 2009). ShakeMaps are produced for each earthquake along with
133 information on date of occurrence, location (latitude, longitude, depth) and
134 magnitude. In total, 377 earthquakes were included (catalog LEQ377), with
135 magnitudes ranging from 5 to 8 and an epicentral intensity (I_0) above or equal to V ,
136 i.e., liable to cause damage (Musson et al., 2010). The observed post-seismic
137 macroseismic intensities would be preferable in this study, due to the inherent
138 uncertainties of the ShakeMaps. However, the ShakeMaps have the advantage of
139 being available for all 377 earthquakes in the catalog (actually the selection criterion
140 for these earthquakes according to Dollet and Guéguen, 2022) and give the spatial
141 variability of ground motion (and thus of the exposure model related to the exposed
142 area for $I_0 > V$) in a uniform way whatever the earthquake.

143

144 Consequences-related data (human and economic) were merged from authoritative
145 international databases (e.g., NOAA, 2018; EM-DAT, 2018; Desinventar, 2018...).
146 For the LEQ377 catalog, the parameters considered are the fatalities F
147 (corresponding to 272 events), injured J (288 events) and direct economic losses $L\$$
148 (288 events). The economic losses were homogenized and adjusted to a US\$
149 reference year. Usually, economic losses should have been adjusted according to a
150 country-specific price index and for the time of the earthquake. This index is not

151 available for each time/country dependent earthquake of the LEQ377 catalogue. In
152 Dollet and Guéguen (2022), an average index was then calculated on consumer
153 prices (CPI) and the construction index (CI) for France, as provided by INSEE
154 (French national institute of statistics and economic studies), and for the USA by the
155 United States Census Bureau (Dollet and Guéguen, 2022). These indexes are
156 available for 2016, which is the reference year used in this study for the adjustment
157 of economic losses. Dollet and Guéguen (2022) showed that the LEQ377 events
158 producing the most cumulative losses (76%) correspond to events of magnitudes
159 between 5.6 and 7.3.

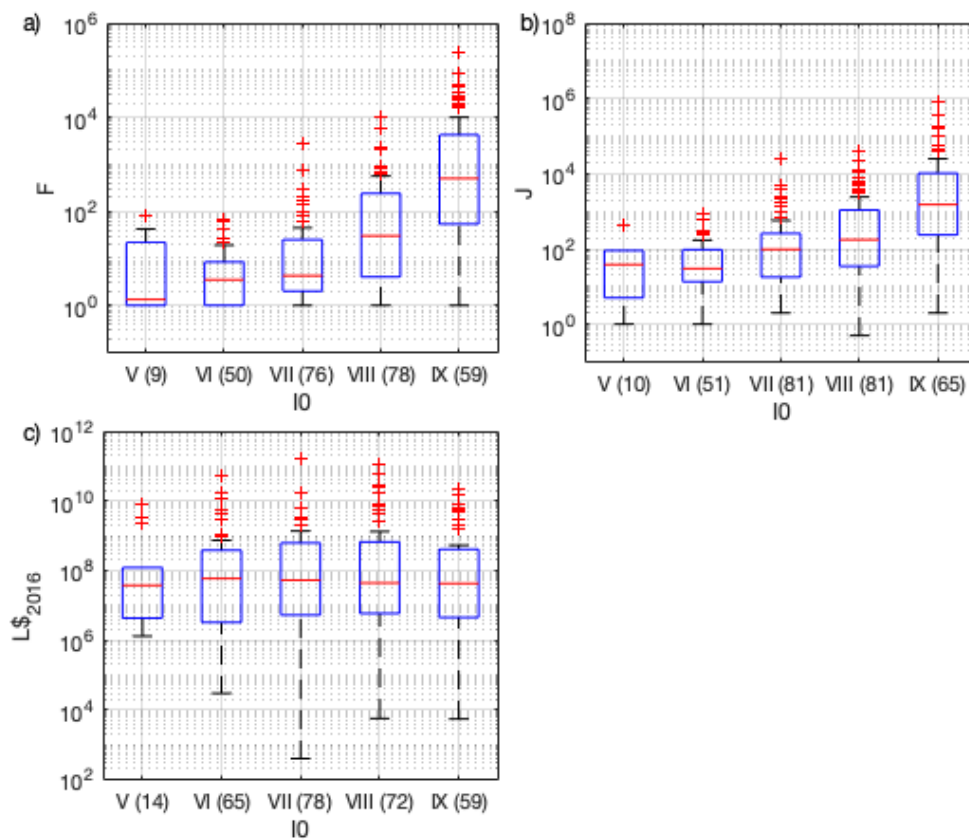
160

161 To get the losses to obey a stationary process, the losses for the year of the
162 earthquake were scaling according to exposure at the time. The exposure data –
163 exposed population and GDP– were calculated and adjusted to the date of the
164 earthquake (Dollet and Guéguen, 2022) using European Commission spatially-
165 distributed demographic data (Eurostat, 2018), with a resolution of 1km, for the year
166 2015. The conversion factor between 2015 and the year of the earthquake was
167 calculated based on the United Nations' population table per country for the period
168 1950-2015 (UN, 2019). Dollet and Guéguen (2022) preferred to calculate exposed
169 GDP per capita in US\$2016 to measure the development of the area concerned;
170 according to Schumacher and Strobl (2011), this provides better statistical
171 significance for loss results. GDP per capita is the country's GDP divided by its
172 number of inhabitants. This index is expressed in US\$ 2010 for each country for the
173 years 1960 to 2018 by the World Bank (World Bank, 2019). Considering GDP to be
174 evenly distributed per country, the GDP per capita is calculated according to the
175 population in the year of the earthquake, then converted into \$2016 using the
176 economic conversion index.

177

178 Figure 1 shows the distribution of social and economic losses by epicentral intensity
179 (I_0) for the LEQ377 database. The earthquakes with I_0 between VII and IX are the
180 largest contributors (in number) to the earthquakes. The social losses (fatalities F
181 and injuries J) and economic losses (L\$) of the earthquakes $I_0 \geq VII$ represent 99%
182 and 83% of total losses in the LEQ377 database, respectively. Events of intensities
183 I_0 between V and VI represent just 1% of total social losses and 17% of economic

184 losses. The dispersion is high, regardless of the intensities and losses considered,
 185 with many atypical values (outside the fourth quartile).



186
 187 **Figure 1.** Social and economic losses by epicentral intensity IO of earthquakes in the
 188 LEQ377 database. a) Number of fatalities (F); b) Number of people injured (J); c)
 189 Economic losses (L\$₂₀₁₆). The number of events per intensity IO is indicated in
 190 brackets.

191
 192 In LEQ377, earthquake losses are associated with the total losses, i.e. considering
 193 direct and indirect losses, distinction rarely provided in the international losses
 194 databases. By consequent, loss values in LEQ377 may include losses from
 195 secondary effects that can introduce a bias in the model (see Daniell et al., 2017 for
 196 the contribution of secondary effects). .

197
 198 **3. Method**

199

200 Figure 2 shows the four steps applied to the LEQ377 database to develop the
201 conversion or loss prediction models used to compile the synthetic database: (1)
202 Magnitude to intensity conversion; (2) Exposed area assessment; (3) Exposure
203 values assessment; (4) Economic and social losses assessment.

204

205 At each step, the model efficiency was evaluated using indicators from the likelihood
206 method proposed by Scherbaum et al. (2004) for ground motion prediction models
207 testing. The quality of the model (“goodness-of-fit”) is obtained by qualifying the
208 adjustment of the model and estimating the extent to which the statistical model
209 hypotheses are met. Scherbaum et al., (2004) thus combined the properties of the
210 residual distributions with a likelihood measurement (LH). The residuals are
211 normalized to obtain a zero mean and unit variance distribution. The quality of a
212 model in relation to the data is ultimately the probability that the absolute value of a
213 random sample of the normalized distribution falls between the absolute value of a
214 particular observation $|z_0|$ and ∞ . Considering the two distribution tails of the error
215 function $\text{Erf}(z)$, the likelihood value $\text{LH}(|z_0|)$ is obtained thus (Scherbaum et al., 2004):

216

$$217 \quad \text{LH}(|z_0|) = \text{Erf}\left(\frac{|z_0|}{\sqrt{2}}, \infty\right) = \frac{2}{\sqrt{\pi}} \int_{|z_0|/\sqrt{2}}^{\infty} e^{-t^2} dt \quad (1)$$

218 Here, we assume that each model developed in steps 1 to 4 can be described by a
219 log-normal distribution. Although the hypotheses of the model correspond exactly for
220 samples taken from a unit variance normal distribution, the samples of the random
221 variable LH are also distributed between 0 and 1. This makes it easy to quantify the
222 adjustment quality using the characteristics of the residual distribution and the
223 properties of the LH values (Scherbaum et al., 2004).

224

225 The absolute values of the mean (Mean-NRES), median (Med-NRES), standard
226 deviation (Std-NRES) of the residuals and of the median of the LH values (Med-LH)
227 thus indicate the central tendency and the diffusion of the distribution. Using these
228 values, Scherbaum et al., (2004) classified the models into three categories of
229 goodness-of-fit (Table 1). The additional category D (unacceptable) applies if the
230 indicators do not meet any criteria of the categories A, B and C. Note that these

231 criteria are determined based on data, i.e., they measure the quality of the model
232 only within the limits of the data available (Scherbaum et al., 2004).

233

234

235

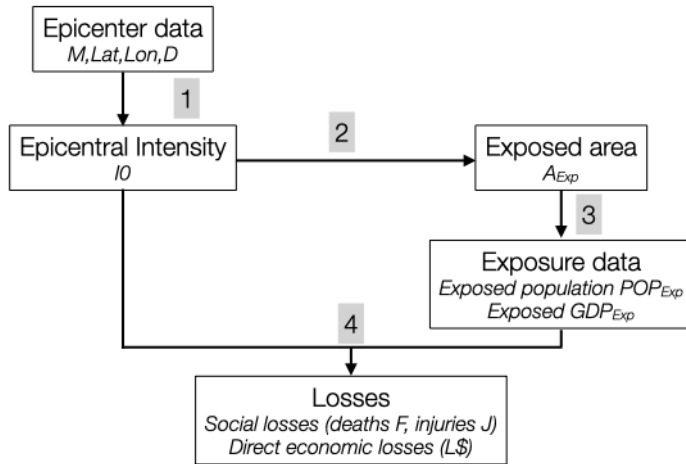
236

237 **Table 1.** Model classification according to the quality criteria defined by Scherbaum
238 et al. (2004). Med-LH: median value of LH; σN : normalized standard deviation of the
239 sample; Mean-NRES, Med-NRES, Std-NRES: mean, median and standard deviation
240 of the residuals.

Category	Acceptance	Med-LH	Mean-NRES	Med-NRES	Std-NRES	σN
C	Low	≥ 0.2	≤ 0.75	≤ 0.75	≤ 0.75	≤ 1.5
B	Middle	≥ 0.3	≤ 0.5	≤ 0.5	≤ 0.5	≤ 1.25
A	High	≥ 0.4	≤ 0.25	≤ 0.25	≤ 0.25	≤ 1.125

241

242



243

244 **Figure 2.** Schematic view of the 4-step process followed to establish the predictive
 245 equation for earthquakes. M, Lat, Lon, D: magnitude, latitude, longitude and depth of
 246 each earthquake. Numbers 1 to 4 correspond to the steps of the process described
 247 in section 3.

248 **3.1 Step 1 – Epicentral intensity prediction equation**

249 The epicentral intensity I_0 of the events in the LEQ377 database is given by the
 250 ShakeMaps. The magnitude (M)/depth (D) pair is converted to I_0 by adjusting an
 251 intensity prediction equation using the functional form as follow (e.g., Atkinson and
 252 Wald, 2007; Bindi et al., 2011):

253

$$254 \quad I_0 = a + bM + c * \log(D) + \sigma \quad (2)$$

255 where a, b and c are the regression coefficients and σ is the standard deviation. Four
 256 relationships are derived, considering different classes of magnitude: [5; 6[, [6; 7[, [7;
 257 8] and [5; 8]. Figures 3 and 4 show the LH and residual distributions for [5; 8] and for
 258 each magnitude class, respectively. Table 2 summarizes the coefficients of the
 259 model equation (Eq. 2), the rank of the equations, and the adjustment quality
 260 indicators according to the LH method. For [5; 8] (Fig. 3), the median of the LH
 261 distribution is 0.29, and the absolute values of the mean and median of the
 262 normalized residuals are 0 and 0.08, respectively (Table 2), with a model ultimately
 263 ranked intermediate (B). The distribution of the normalized residuals (Figure 3a)
 264 shows that the variance of the sample tested is greater than the model variance.

265

266 **Table 2.** Rankings of different epicentral intensity prediction equation to model the
 267 LEQ377 dataset of Dollet and Gueguen (2022).

M Ranking	Reg. coef Eq. 2	Rank	Med-LH	Med-NRES	Mean-NRES	Std-NRES	No. of events
[5-8]	a 1.35	B	0.29	0.08	0	1.41	268
	b 1.22						269
	c -0.69						377
	σ 0.8						
[5-6[a 2.19	C	0.19	0.03	0	2.56	270
	b 0.89						85
	c -0.30						
	σ 0.72						
[6-7[a 0.77	B	0.24	0.18	0	1.48	271
	b 1.43						272
	c -0.95						187
	σ 0.82						273
[7-8]	a 5.40	C	0.20	0.03	0	1.67	274
	b 0.64						275
	c -0.64						105
	σ 0.72						277
							278

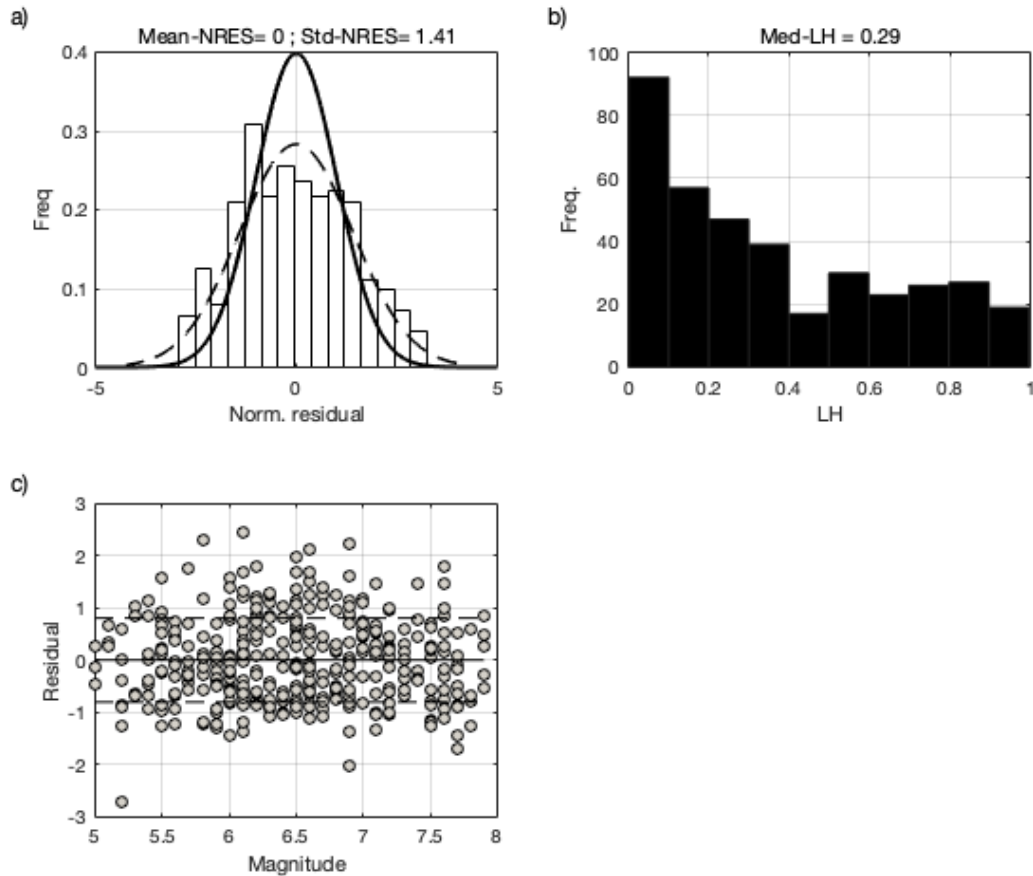
279

280

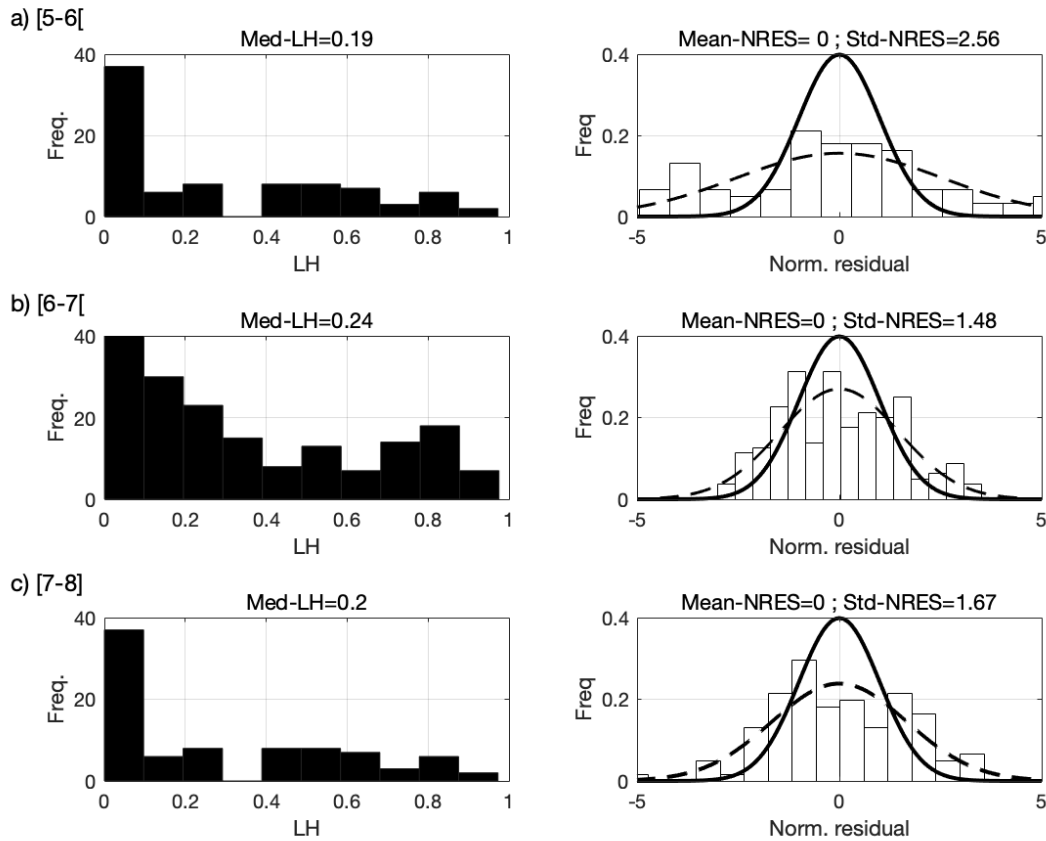
281 For the other magnitude ranges (Fig. 4, Tab. 2), the median of the LH distribution is
 282 0.19, 0.24 and 0.20 for [5-6[, [6-7[and [7-8], respectively. Considering the absolute
 283 value of the mean (0) and the median of the normalized residuals (0.03) for [5-6[and
 284 [7-8], the models are ranked C. In conclusion, for the sake of simplicity, we will use
 285 the model [5-8] (rank B) equation without distinguishing the magnitude ranges.

286

287



288
 289 **Figure 3.** Distribution of residuals (a), corresponding LH values (b) and residuals as
 290 a function of magnitude (c) for the earthquakes with magnitude ranges [5; 8] from the
 291 LEQ377 database. The mean and standard deviation values of the residual
 292 distribution and the median value of the resulting LH-value distribution are given at
 293 the top of the panel (a) and (b) respectively. The two distribution functions in (a)
 294 indicate the unit variance normal distribution (continuous) and the actual residual
 295 distribution (dashed). The continuous and dashed horizontal lines in (c) indicate
 296 mean +/-std of the residual distribution as a function of magnitude.



297
 298 **Figure 4.** Same as Figs. 3a and 3b for magnitude ranges (a) [5-6[; (b) [6-7[; (c) [7-8].

299
 300 **3.2 Step 2 – Prediction of exposed areas as a function of I0**

301
 302 To estimate the exposure values, the exposed areas for each macro-seismic
 303 intensity are given by the ShakeMaps of the LEQ377 events. As already confirmed
 304 by Dollet and Guéguen (2022), the higher the magnitude (M)/depth(D) ratio, the
 305 higher the epicentral intensity I0 and the larger the exposed area for each level of
 306 macroseismic intensity (e.g., among others Levret and al., 1994; Bakun and Scotti,
 307 2006). Using exposed areas, the epicentral distance and depth is then considered.
 308 Without prior functional forms known, we started by testing two conventional forms
 309 taken from seismic motion (Douglas, 2003) or intensity (Bakun and Scotti, 2006)
 310 predictions:

311

312 $\log (A_{\text{exp}/I}) = a(I) * I_0 + b(I) * D + c(I) * \log(D)$ (3a)

313 $\log (A_{\text{exp}/I}) = a(I) * D + b(I) * \log(D) + \sigma$ (3b)

314 where $A_{\text{exp}/I}$ is the cumulative exposed area in km^2 (i.e., $A_{\text{exp}/I} = \sum_I^{I_0} A_{\text{exp}/i}$ for
 315 macroseismic intensity $I > V$), a , b and c are the coefficients of the model, σ is the
 316 standard deviation, and D is distance in km. We chose to consider cumulative area,
 317 because the losses reported in LEQ377 are not given by intensity. For every I_0 , I
 318 range from V to I_0 .

319

320 Without going into further detail, the model (Eq. 3a) does not meet the LH criteria and
 321 the quality classes are low (C) to unacceptable (D). Only equation 3b will therefore
 322 be discussed hereinafter.

323

324 The coefficients a , b , and c of equation 3b depend upon macroseismic intensity: we
 325 therefore developed 15 relationships calculating the cumulative exposed area for
 326 each macroseismic intensity and for I_0 between $[V; IX]$ (Tab. 3). With one exception,
 327 the models were all ranked A or B. For example, Figure 5 shows for $I_0=VII$ the
 328 normalized distribution of residuals (Fig. 5a), the corresponding LH values (Fig. 5b)
 329 and the value of the residuals as a function of depth (Fig. 5c) for each macroseismic
 330 intensity $I \leq I_0$. For $I = V$ (i. e., $\sum_V^{VII} A_{\text{exp}/i}$) to $I = VII$ (i. e., $A_{\text{exp}/VII}$), the mean residual
 331 and the standard deviation of the distribution are 0.1, 0, 0, and 0.75, 0.87 and 1.65,
 332 respectively (Table 3). Figure 5c shows an under-estimation of the exposed areas for
 333 $D > 30\text{km}$ (Fig. 5c). The distribution medians of the LH values (Fig. 5b) are 0.55, 0.51
 334 and 0.26 for $I=V$, $I=VI$ and $I=VII$, respectively. Bearing in mind that the absolute value
 335 of the median of the normalized residuals is 0.06 for $I=V$, 0.02 for $I=VI$ and 0.05 for
 336 $I=VII$, the exposed area prediction model for $I_0=VII$ ranked A (Tab. 3).

337

338 Similarly, for $I_0=VI$ (Fig. 6), the median value of LH is 0.69 and 0.46 for $I=V$ and VI ,
 339 respectively. The absolute values of the mean and the mean of the normalized
 340 residuals are 0.2 and 0.04 for $I=V$ and 0.2 and 0.18 for $I=VI$, respectively. Finally, the
 341 exposed area model for $I_0=VI$ ranked A (Tab. 3).

342

343 Note that the normalized residual distributions (Fig. 5a and 6a) are narrower than a
344 unit normal distribution. The sample variance is therefore smaller than that of the
345 model, characterized with bias in terms of mean (Scherbaum and al., 2004). The
346 median of LH is above 0.5 and the associated LH distributions are asymmetrical, i.e.,
347 the models under-estimate the cumulative exposed area. The distribution of LH
348 values appears asymmetrical for all models when intensity I is strictly less than I₀,
349 with an LH median value above 0.5. When macroseismic intensity I is I₀, the
350 frequency of the low values of LH increases and the median of the LH distribution
351 falls below 0.5. According to Table 3, the exposed area models for each I₀ rank
352 medium (B) to high (A), except for $A_{\text{exp}/\text{VIII}}$ for I₀ = VIII, although we have no
353 explanation for this.

354

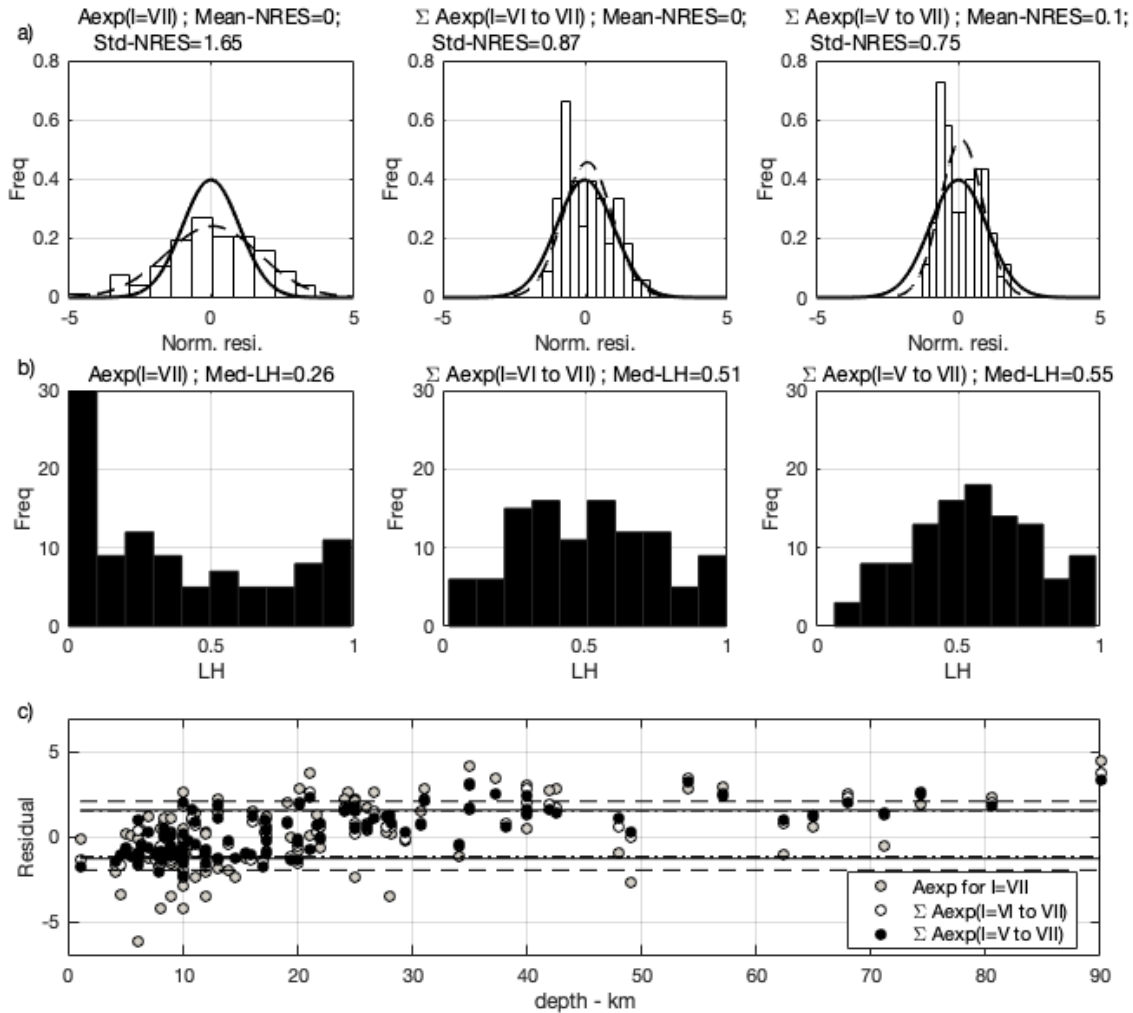
355 **Table 3.** Rankings of the relationships for cumulative exposed areas as a function of
356 I₀ to model the LEQ377 dataset of Dollet and Gueguen (2022).

I ₀	A_{exp}	Reg. coef Eq. 3b		Rank	Med- LH	Med- NRES	Mean- NRES	Std- NRES S	Nbr. of events
		a	b						
V	$A_{\text{exp}/\text{V}}$	-0.012	1.96	B	0.27	0.24	0.09	1.50	41
VI	$\sum_{\text{V}}^{\text{VI}} A_{\text{exp}/i}$	-0.037	3.18	A	0.69	0.04	0.20	0.63	112
	$A_{\text{exp}/\text{VI}}$	-0.031	2.25	A	0.46	0.18	0.23	1.18	
VII	$\sum_{\text{V}}^{\text{VII}} A_{\text{exp}/i}$	-0.098	4.20	A	0.55	0.06	0.10	0.75	108
	$\sum_{\text{VI}}^{\text{VII}} A_{\text{exp}/i}$	-0.069	3.45	A	0.51	0.02	0.09	0.87	
	$A_{\text{exp}/\text{VII}}$	-0.030	2.19	B	0.26	0.05	0.06	1.65	
VIII	$\sum_{\text{V}}^{\text{VIII}} A_{\text{exp}/i}$	-0.090	4.43	A	0.68	0.24	0.18	0.60	83
	$\sum_{\text{VI}}^{\text{VIII}} A_{\text{exp}/i}$	-0.069	3.84	A	0.63	0.23	0.16	0.65	
	$\sum_{\text{VII}}^{\text{VIII}} A_{\text{exp}/i}$	-0.050	3.18	A	0.59	0.15	0.15	0.75	
	$A_{\text{exp}/\text{VIII}}$	-0.041	2.12	C	0.22	0.26	0.11	1.62	
IX	$\sum_{\text{V}}^{\text{IX}} A_{\text{exp}/i}$	-0.34	6.49	A	0.72	0.20	0.19	0.42	33
	$\sum_{\text{VI}}^{\text{IX}} A_{\text{exp}/i}$	-0.27	5.64	A	0.76	0.14	0.18	0.49	
	$\sum_{\text{VII}}^{\text{IX}} A_{\text{exp}/i}$	-0.21	4.87	A	0.78	0.08	0.18	0.56	

$\sum_{VIII}^{IX} A_{exp/i}$	-0.14	3.93	A	0.78	0.02	0.17	0.69
$A_{exp/VIII}$	0.021	1.85	A	0.55	0.15	0.02	1.40

357

358



359

360

361

362

363

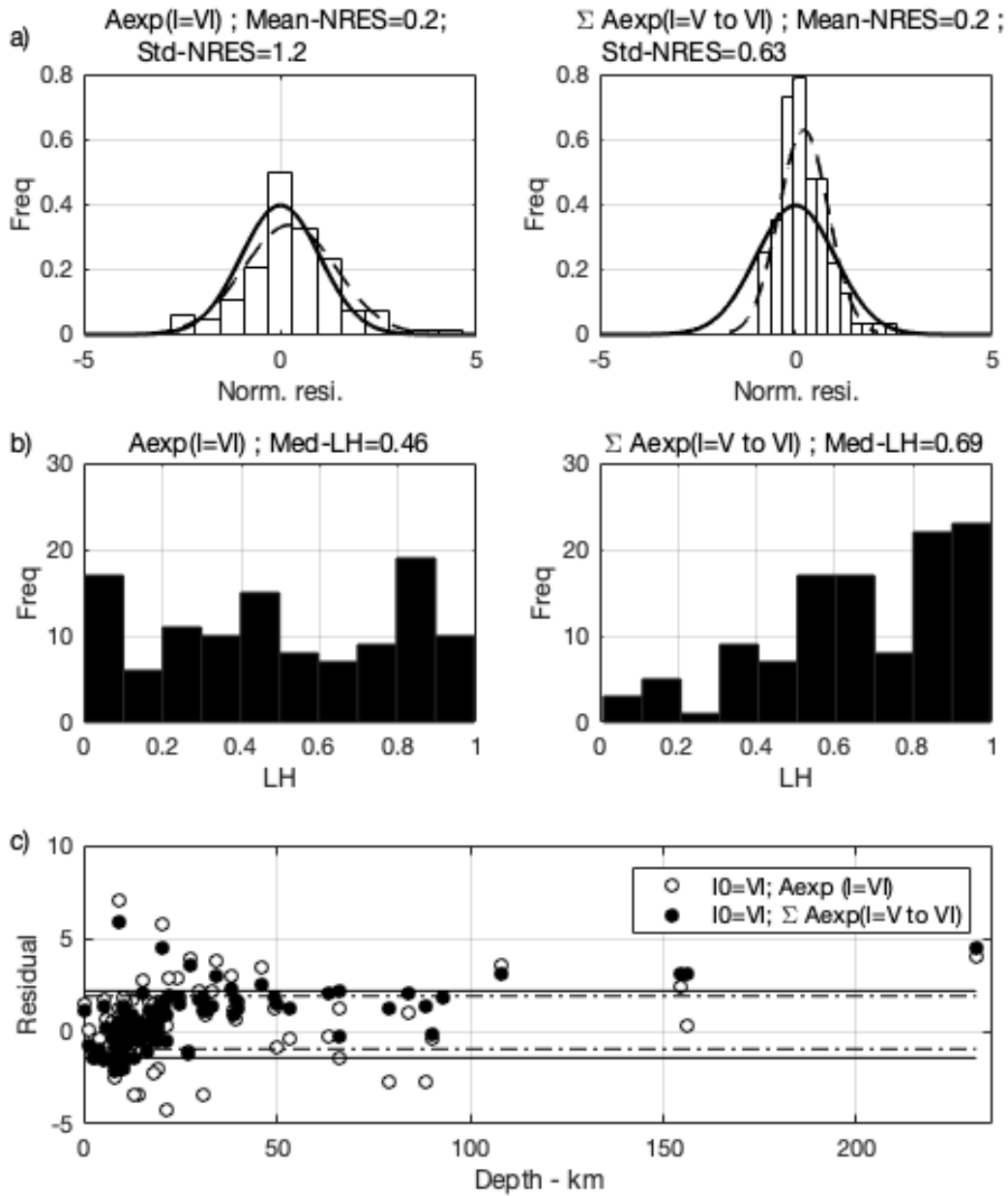
364

365

366

367

Figure 5. Distribution of residuals (a), corresponding LH values (b) and residuals as a function of depth (c) for I0=VII earthquakes in the LEQ377 database. The mean and standard deviation values of the residual distribution (a) and the median value of the resulting LH-value distribution (b) are given at the top of the panels. The two distribution functions in (a) indicate the unit variance normal distribution (continuous) and the actual residual distribution (dashed). The horizontal dashed lines in (c) indicate \pm -std of the residual distribution as a function of depth.



368
369 **Figure 6.** Same as Fig. 5 for I0=VI

370
371

372 3.3. Step 3 – Loss models

373

374 For seismic losses, it is common practice to consider a model with the following
375 functional form (e.g., Heatwole and Rose, 2013; Guettiche and al., 2017):

376

377
$$\log_{10}(L) = c_1 * \log_{10}(I_0) + c_2 * \log_{10}(X_2) + \dots + c_i * \log_{10}(X_i) + \sigma \quad (4)$$

378

379 where $\log_{10}(L)$ represents the logarithmic function of the economic or human
380 consequences, c_i are the regression coefficients and i is the number of variables X .
381 This step requires consideration of the exposure variables (exposed population and
382 exposed GDP per capita) for each macroseismic intensity, already calculated for
383 LEQ337 (Dollet and Guéguen, 2022) based on (1) the georeferenced population grid
384 2015 (Eurostat, 2018) and the demographic growth conversion factor (UN, 2019); (2)
385 GDP per capita of the countries affected by the earthquake (Word Bank, 2019) in
386 US\$ in the year of the earthquake, converted to US\$(2016) using the average
387 economic index proposed by Dollet and Guéguen (2022). To test the models, only
388 the overall losses associated with each earthquake are given, with no distinction of
389 losses per macroseismic intensity (not available in the international loss databases)
390 but considering exposure for each macroseismic intensity.

391

392 **3.3.1 Prediction models for economic losses (L\$2016) as a function of I0 and** 393 **GDPexp**

394

395 In the LEQ377 database, economic losses are indicated for 288 earthquakes. We
396 derived the model (called DOL22) from Eq. 4, considering cumulative GDP per capita
397 calculated as the sum of exposed GDP per capita for each macroseismic intensity I
398 between $[X_i=I; i=V \text{ to } I_0]$. Figure 7a shows the distribution of residuals and LH values
399 for the derived model, compared with two existing models produced by Guettiche et
400 al. (2017) (GUE17, Fig. 7b) and Heatwole and Rose (2013) (HEA13, Fig. 7c):

401

$$402 \text{ GUE17} \quad \log_{10}(L) = c_1 * \log_{10}(I_0) + c_2 * \log_{10}(\text{GDP}_{\text{expTotal}}) + c_3 \quad (5a)$$

$$403 \text{ HEA13} \quad \log(L) = c_1 * \log(\text{Mag}) + c_2 * \log(\text{Pop}_{\text{expTotal}}) + c_3 \quad (5b)$$

404

405 The LH values of the DOL22 model (Table 4) give a median of 0.30, and the absolute
406 values of the mean and the median of the normalized residuals are 0.03 and 0.02,
407 respectively (model rank B). Note that the distribution of normalized residuals (Fig.
408 7a, left panel) has a higher variance than the model variance, the low values of LH
409 have an increasing frequency and the LH distribution has a median value that falls

410 below 0.5. The associated mean residual is 0.0, with a standard deviation of the
 411 distribution of 1.51.

412

413 The coefficient c_1 of the DOL22 model (Eq. 4, Table 4) is high, indicating that each
 414 increase in I_0 causes a large increase in economic losses. This suggests that the
 415 economic losses due to earthquakes are much more dependent on the parameter
 416 defining the hazard than on the parameters defining exposure.

417

418 **Table 4.** Classification of economic loss prediction models (losses in million
 419 US\$2016) DOL22 (this study), Guettiche et al., (2017, GUE17) and Heatwole and
 420 Rose (2013, HEA13). The coefficients are those of equations 4 and 5.

I_0	Reg. coef Eq. 4 and 5	Rank	Med-LH	Med- NRES	Mean- NRES	Std- NRES
DOL22	c_1					
	c_2					
	c_3					
	c_4	B	0.30	0.02	0.03	1.51
	c_5					
	c_6					
	σ	1.21				
GUE17	c_1					
	c_2	A	0.52	0.52	0.51	0.77
	c_3					
	σ					
HEA13	c_1					
	c_2	A	0.51	0.13	0.12	1.00
	c_3					
	σ					

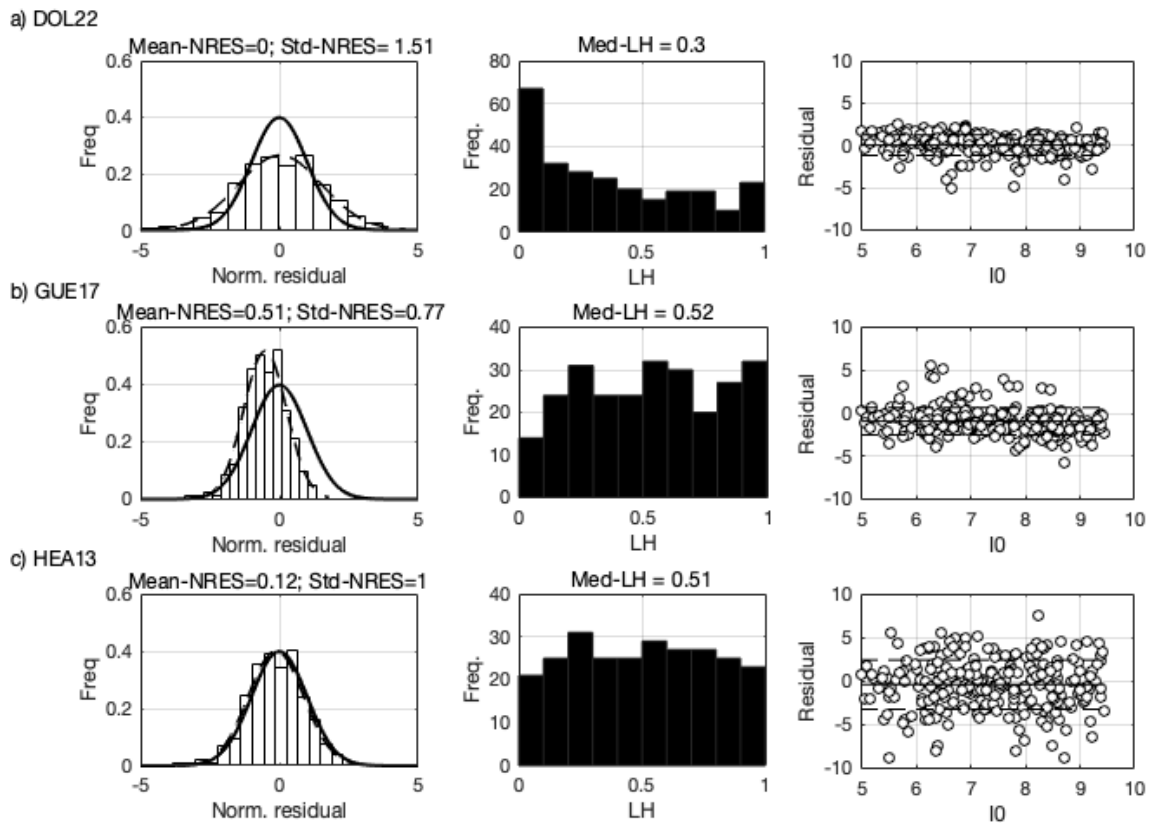
421

422

423 Models GUE17 and HEA13 are ranked A (Tab. 4). However, Figure 7 shows a highly
 424 dispersed normal law for HEA13 ($\mu=-0.4$, $\sigma=2.82$) (Fig. 7c) and GUE17 ($\mu=-0.93$,
 425 $\sigma=1.59$) (Fig. 7b), although $\mu=0$ and $\sigma=1.21$ for model DOL22 (Figure 9a). Thus,
 426 although our model is ranked below GUE17 and HEA13, the consideration of local
 427 exposure improves the distribution of economic loss residuals.

428

429



430
 431 **Figure 7.** Distribution of residuals (left panel), corresponding LH values (middle
 432 panel) and residuals as a function of I0 (right panel) for the economic losses of the
 433 LEQ377 database, considering DOL22 (a), GUE17 (b), and HEA13 (c). Same
 434 symbols and legends as in Fig. 5.

435
 436 **3.3.2. Prediction models for fatalities F as a function of I0 and POPexp**

437
 438 Figure 8 and Table 5 summarize the results ranking of model DOL22 (Fig. 8a) and
 439 models GUE17 (Figure 8b) and BAD05 (Badal et al. 2005; Figure 8c) for the
 440 prediction of fatalities. The equations of models GUE17 and BAD05 are:

441
 442 GUE17 $\log_{10}(F) = c_1 * \log_{10}(I0) + c_2$ (6a)

443 BAD05 $\log(F) = c_1(\text{Pop density}) * M + c_2(\text{Pop density})$ (6b)

444
 445 The median of the LH value distribution (0.26), and the absolute values of the mean
 446 and the mean of the normalized residuals (0 and 0.39) rank DOL22 as intermediate
 447 (B). Figure 9a shows that the variance of the tested sample is higher than the
 448 variance of the model. The positive mean residual indicates that the model prediction

449 model under-estimates the number of fatalities. This under-estimation is most
 450 obvious for intensities I_0 greater than or equal to VIII (Fig. 8a, right panel). The model
 451 adjustment could be improved with loss data for each macroseismic intensity, but
 452 these are not currently available in the international databases. Unlike the economic
 453 model, the coefficient values c_i (in absolute value) rank the same for I_0 and for the
 454 variables related to exposure, suggesting that human losses depend as much on the
 455 parameter related to the hazard event as on the parameter related to exposure.

456

457 **Table 5.** Classification of prediction models for number of fatalities DOL22 (this
 458 study), GUE17 (Guettiche et al., 2017) and BAD05 (Badal et al., 2005). For DOL22,
 459 the coefficients c_i ($i>1$) correspond to the exposure values X_i (with $i \in [V; I_0]$). For
 460 BAD05, coefficients c_1 and c_2 depend on population density and are not indicated in
 461 the table (see Tab. II in Badal et al. 2005).

462

I_0	Reg. coef Eq. 4 and 6	Rank	Med-LH	Med- NRES	Mean- NRES	Std- NRES	
DOL22	c_1	-0.37	B	0.26	0.39	0	
	c_2	0.18					
	c_3	0.02					
	c_4	0.08					
	c_5	0.24					
	c_6	0.15					
	σ	0.89					
GUE17	c_1	12.8	C	0.24	0.31	0.09	
	c_2	-9.85					
	σ	0.89					
BAD05	σ	1.72	D	0.12	1.42	1.09	1.20

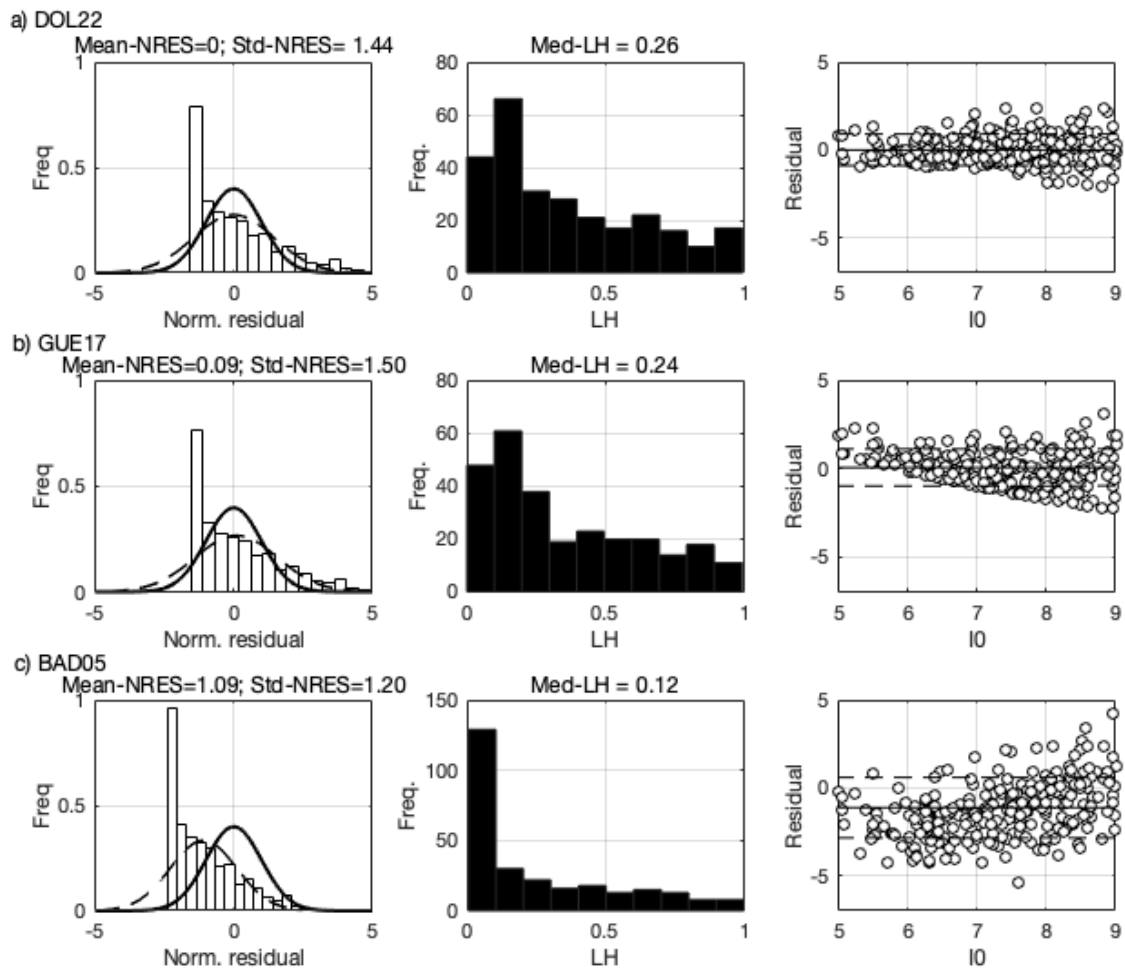
463

464

465 Models BAD05 and GUE17, which consider overall exposure, rank much lower (D
 466 and C, respectively). In particular, $\mu=-1.13$ and $\sigma=1.72$ for BAD05, $\mu=0.08$ and
 467 $\sigma=1.06$ for GUE17 (in comparison with $\mu=0$ and $\sigma=0.89$ for DOL22).

468

469



470
 471 **Figure 8.** Same as Fig. 7 for fatalities and considering DOL22 (a), GUE17 (b) and
 472 BAD05 (c).

473
 474 **3.3.3. Prediction model for number of people injured as a function of IO and**
 475 **POPexp**

476
 477 As for the number of fatalities, our hypothesis is that the variables of exposure per
 478 intensity improve the prediction of the number of people injured. Figure 9 and Table 6
 479 summarize the results that rank the model derived in this study (Fig. 9a, DOL22) and
 480 compared with the Guettiche et al. (2017) model (Fig. 9b, GUE17) for injuries,
 481 according to the equation:

482
 483 GUE17
$$\log_{10}(J) = c_1 * \log_{10}(IO) + c_2 + \sigma \quad (7)$$

484

485 where J is the number of people injured. The median of the LH value distribution
 486 (0.31), and the absolute values of the mean and median of the normalized residuals
 487 (0 and 0.13) rank DOL22 as intermediate (B). The positive mean residual indicates
 488 that the model under-estimates the number of people injured, which does not appear
 489 to depend upon intensity I_0 .

490

491 **Table 6.** Classification of the prediction models for the number of people injured:
 492 DOL22 (this study) and GUE17 (Guettiche et al., 2017). For DOL22, the coefficients
 493 c_i ($i > 1$) correspond to the exposure values X_i (with $i \in [V; I_0]$).

I_0	Reg. coef Eq. 4 and 6	Rank	Med-LH	Med- NRES	Mean- NRES	Std- NRES
DOL22	c_1					
	c_2					
	c_3					
	c_4	B	0.31	0.13	0	1.51
	c_5					
	c_6					
	σ	0.86				
GUE17	c_1	C	0.27	0.03	0.18	1.72
	c_2					
	σ					0.78

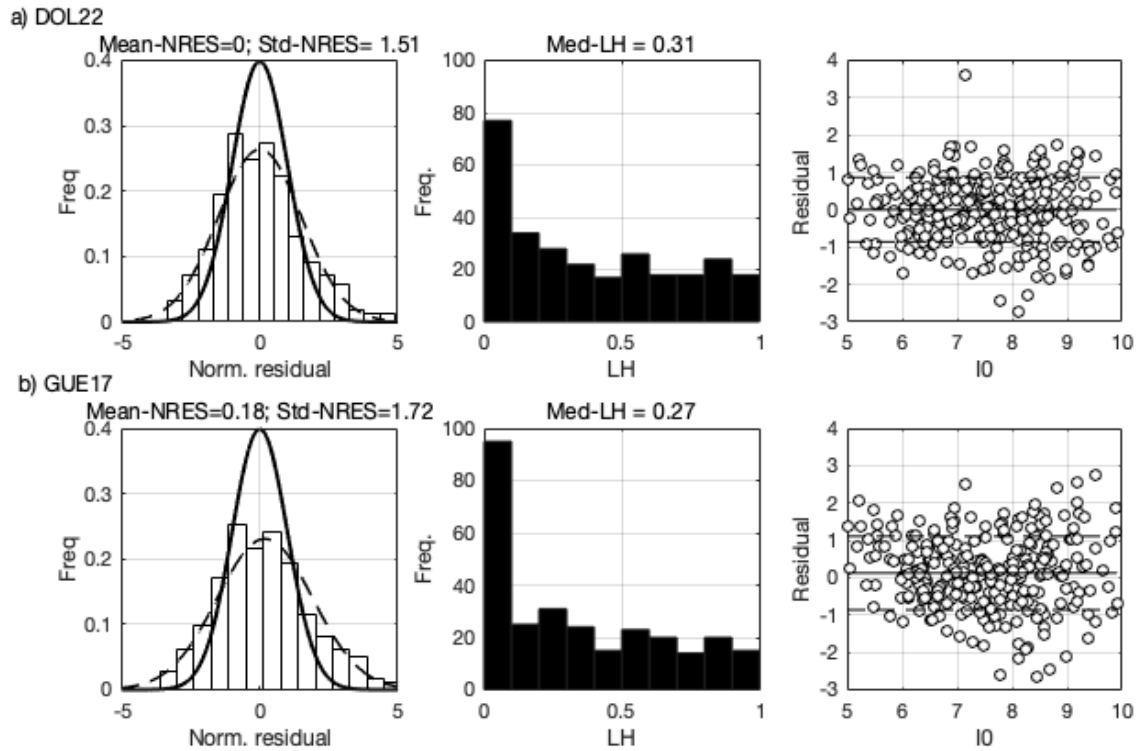
494

495

496 Figure 9 confirms the hypothesis that consideration of the exposed population per
 497 intensity improves the prediction of the number of people injured, as model GUE17 is
 498 ranked C. The residuals of models DOL22 and GUE17 (Fig. 9, right panel) are
 499 normally distributed with a zero mean and unit variance ($\mu=0$ and $\sigma=0.86$ for model
 500 DOL22 and $\mu=0.12$ and $\sigma=0.99$ for model GUE17). The improvement obtained by
 501 considering exposure per intensity is visible on the dispersion.

502

503



504
505 **Figure 9.** Same as Fig. 7 for injuries and considering DOL22 (a) and GUE17 (b).

506

507 **4. Construction of the synthetic database**

508

509 To compensate for the lack of loss data for low magnitudes, we built a database
510 according to the procedure defined in Fig. 2. First, we calculated I0 values according
511 to Eq. 2 from M and the locations in the ISC-GEM catalog (2019), which is
512 considered complete for $M > 5$ for the period 1900-2015 (Di Giacomo et al., 2018). A
513 total of 17,721 seismic events with $I0 \geq V$ (i.e., with possible losses), $M \in [5.5; 8[$ over
514 the period 1967-2015 were considered.

515

516 Next, the Aexp values derived from Eq. 3b were calculated for all the earthquakes,
517 supposing an equivalent concentric circular surface area for each intensity. Only the
518 earthquakes whose Aexp $I > V$ affected a populated area were retained, population
519 being estimated by crossing Aexp $I > V$ with the georeferenced population table 2015
520 (European Commission, 2019) for each event. 7,515 events (42%) were thus
521 retained, forming the dataset herein referred to as ISC7515, with the following
522 distribution of number of events per intensity: [V-VI]: 1,797 events; [VI-VII]: 4,220
523 events; [VII-VIII]: 1,289 events; [VIII-IX]: 196 events; [IX-X]: 13 events.

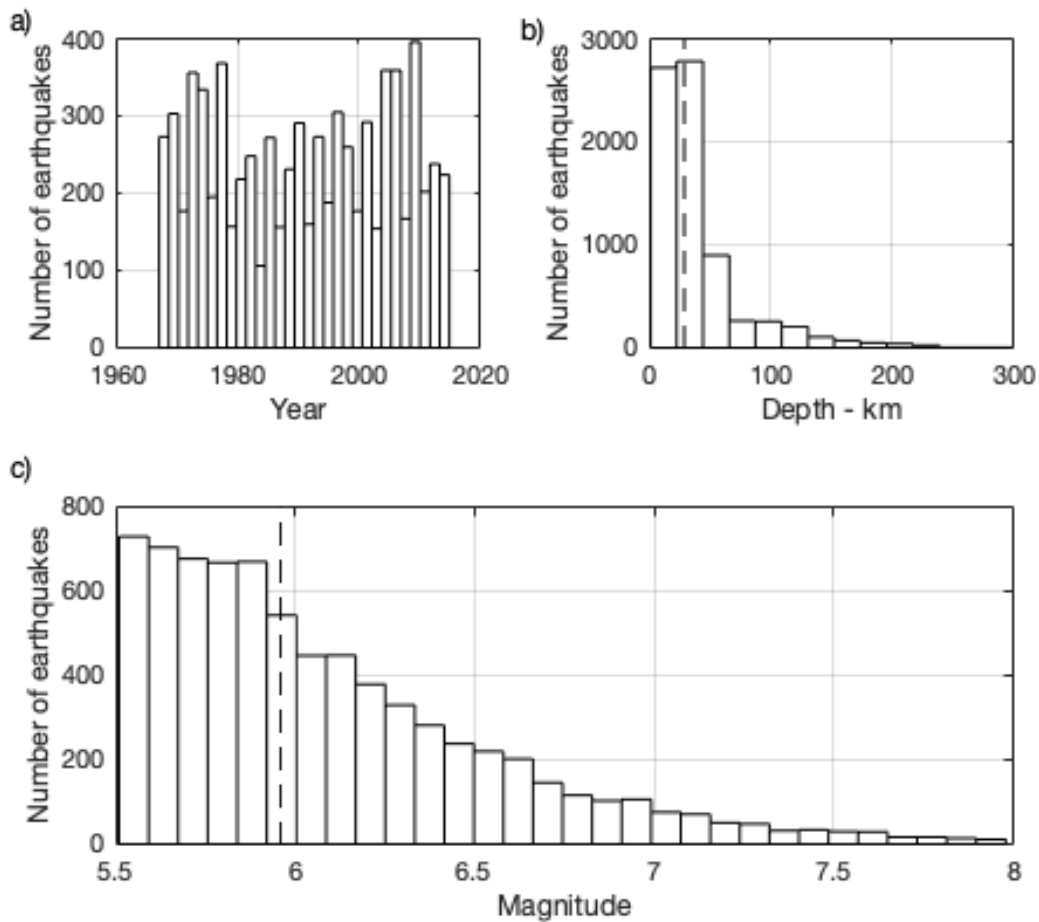
524

525 Finally, the exposed GDP per intensity was calculated according to the method
526 proposed by Dollet and Guéguen (2022) using GDP per capita for the country
527 affected (World Bank, 2019) in US\$, and the exposed population in 2010, converted
528 to the year 2016 using the average economic index. For earthquakes affecting
529 several countries, exposure values in each country are considered and merged
530 accordingly.

531

532 Figure 10 shows the distribution of the number of earthquakes per year, by depth and
533 by magnitude, in the ISC7515 database. As for the LEQ377 database of earthquakes
534 and losses observed (Dollet and Guéguen, 2021), a few noteworthy trends are visible
535 for ISC7515 (Fig. 10): these are the superficial earthquakes that can make the
536 largest contribution to losses; most of the earthquakes (68%) able to cause losses
537 according to the selection criteria applied by this study are events of moderate
538 magnitude, between [5.5 and 6.4].

539



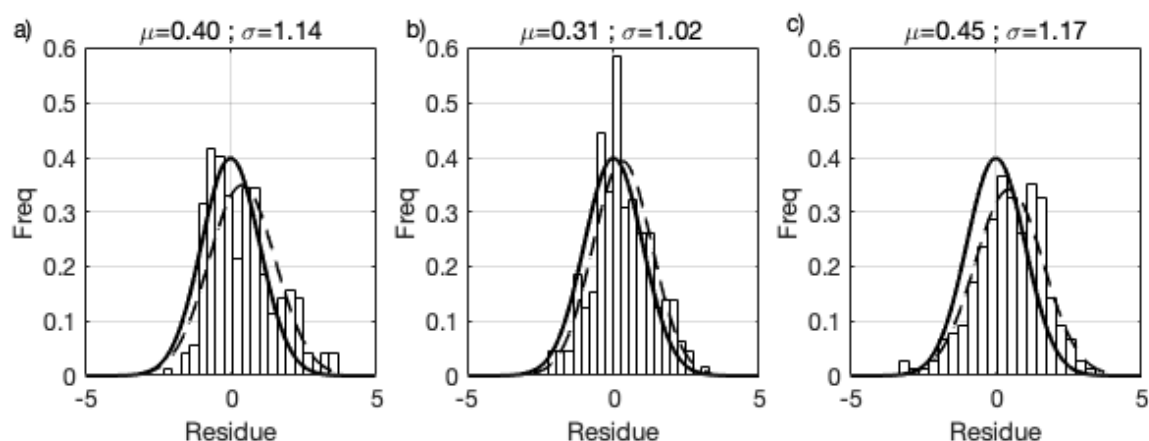
540 **Figure 10.** Distribution of the number of earthquakes in database ISC7515 a) by
 541 year, b) by depth, c) by magnitude. The black dashed lines on b) and c) represent the
 542 median values of depth (28.9 km) and magnitude (6.0).
 543

544
 545 Losses were finally calculated using the Eq. 4 models with the regression coefficients
 546 by intensity I0 of Tables 4 to 6. Concerning GDP per capita, only 6,809 seismic
 547 events were considered, as the World Bank tables (2019) do not provide GDP values
 548 for some exposed countries.

549
 550 **4.1 Test on LEQ377**

551
 552 The distribution of the synthetic loss residuals for the LEQ377 events is given in Fig.
 553 11. The synthetic data under-estimate the probable losses. The distributions of the
 554 residuals for social and economic losses follow a normal value distribution $\mu = 0.4$; σ
 555 $= 1.14$ for F, $\mu = 0.31$; $\sigma = 1.02$ for J and $\mu = 0.45$; $\sigma = 1.17$ for L\$. Two hypotheses

556 might explain this under-estimation: (1) distribution of losses related to damage to
 557 buildings not considered in this study (because of missing information in the
 558 international database) although the losses are highly correlated with structural
 559 collapse (e.g., Coburn and Spence, 2003; Riedel and al., 2014; 2015; Guettiche and
 560 al., 2017); (2) high uncertainty related to the evaluation of exposed areas per
 561 intensity, with consequences on the estimations of exposed populations and GDP.
 562 These uncertainties might also include the values given in the ShakeMaps.
 563



564 **Figure 11.** Distribution of the residuals of (a) fatalities, (b) number of people injured,
 565 and (c) economic losses of seismic events in the LEQ377 database. Residue =
 566 $\log_{10}(\text{obs}) - \log_{10}(\text{pred})$.
 567

568
 569 **4.2 Synthetic losses**

570
 571 Table 7 summarizes the statistical indicators associated with the social and economic
 572 losses calculated from the synthetic database ISC7515. Total economic losses
 573 represent US\$(2016) 87.736 billion, with a mean loss of around US\$(2016) 12.88
 574 million. The Kurtosis are very high, i.e., the distribution tails include more
 575 observations than in a Gaussian distribution, and there are a lot of values a long way
 576 from the mean. This means that the strongest ($M \geq 7$) and low-probability earthquakes
 577 contribute significantly to economic losses (64%), and social losses (44% for fatalities
 578 and 29% for people injured). However, the cumulative losses for earthquakes
 579 between 5.5 and 7.0 (i.e., 95% of ISC7515 events) that correspond to weak-to-
 580 moderate earthquakes, contribute very significantly to the global seismic losses: they

581 represent 36% of all economic losses, 56% of all fatalities, and 71% of people
 582 injured. Note also that weak-to-moderate earthquakes may cause higher cumulative
 583 social losses but lower cumulative economic losses than stronger magnitude
 584 earthquakes.

585

586 **Table 7.** Economic losses L\$ (US\$2016), number of fatalities and people injured
 587 calculated for the events in the synthetic database ISC7515

	Fatalities	Injuries	Economic L\$2016
Total value	54,713	366,559	87,736,086,272
Mean	7	49	12,885,312
Standard deviation	79.7	198.1	145,854,342
Kurtosis	3,379.9	2,145.8	1,775.2
Median	3.5	28.5	1,950,616
Number of events	7,515	7,515	6,809

588

589

590

591 **5. Annual rate of exceedance of losses**

592

593 Assuming a complete synthetic loss catalog, we then derived an exceedance model
 594 for the 7,515 seismic events between 1967 and 2018, according to the following
 595 functional form inspired by the seminal Guttenberg-Richter model:

596

$$597 \log_{10}N(Y > X) = a - b * \log_{10}X \quad (9)$$

598 where $N(Y>X)$ represents the number N of earthquakes with a ratio Y of social losses
 599 to exposed population (F/POP_{exp} or J/POP_{exp}) or economic losses ($L\$/GDP_{exp}$)
 600 greater than or equal to a given loss X . Note that Eq. 9 predicts losses with no upper
 601 limit. However, physical constraints related to exposure (population and GDP) make
 602 this unrealistic, i.e., in the spirit of the maximal magnitude of the Guttenberg-Richter
 603 model defined by the finite size of the source faults of a given region. For this reason,
 604 limited loss models, called bounded loss exceedance models, are computed with the
 605 number of deaths and injuries limited by the value of the exposed population and the
 606 economic losses limited by twice the exposed GDP.

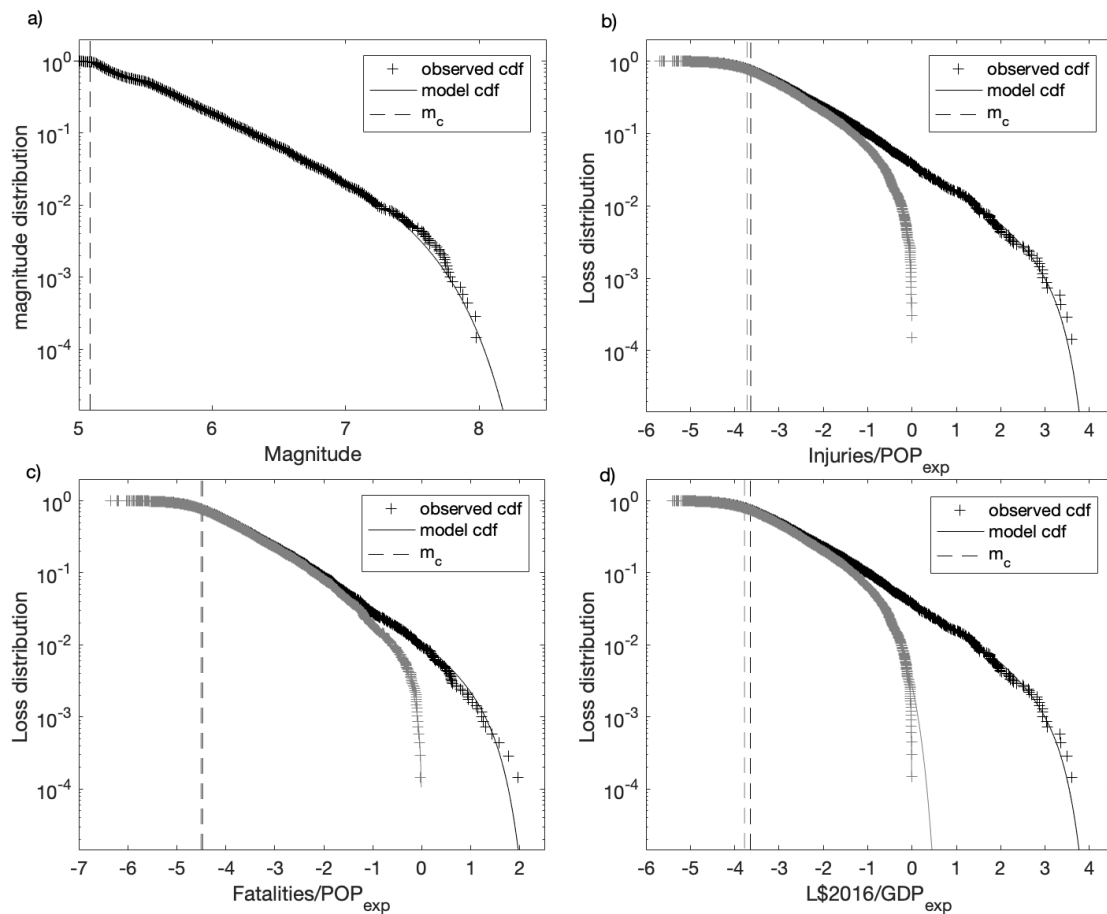
607 Figure 12 represents the cumulative distribution of the unbounded and bounded
 608 synthetic losses, computed following the maximum likelihood estimation-based
 609 method proposed by Ogata and Katsura (1993). Completeness value L_c and
 610 regression coefficients (Eq. 9) are given in Table 8.

611 **Table 8.** Completeness and regression coefficients (Eq. 9) of the synthetic database
 612 (from Ogata and Katsura 1993 method).

	Fatalities <i>Boun./Unboun.</i>	Injuries <i>Boun./Unboun.</i>	Economic <i>Boun./Unboun.</i>	Magnitude
Completeness L_c or M_c	$3.3 \cdot 10^{-5}/3.1 \cdot 10^{-5}$	$2.3 \cdot 10^{-4}/1.9 \cdot 10^{-4}$	$2.3 \cdot 10^{-4}/1.7 \cdot 10^{-4}$	5.08
b	0.40/0.39	0.36/0.33	0.36/0.31	0.77

613
 614 The b values lesser than 1 indicate the relative ratio of small and large losses, which
 615 confirms the preponderance of small-to-weak cumulative losses in the overall losses.
 616 The completeness values for bounded and unbounded synthetic losses (L_c) do not
 617 show a significant difference, while the b values changes do. The long return period
 618 model values are constrained by a small number of earthquakes due to the relatively
 619 short period of the considered catalog. Therefore, their impact on intermediate loss
 620 values (i.e., short return period) remains limited and confirms the relevant information
 621 provided by this model for weak-to-moderate earthquakes.

622



623
 624 **Figure 12.** Frequency distribution of events (cumulative distribution) estimated
 625 following the method proposed by Ogata and Katsura (1993) for (a) the magnitude of
 626 the events, (b) the injuries and (c) fatalities normalized by the exposed population,
 627 and (d) the economic losses normalized by the exposed GDP along with bounded
 628 (gray) and unbounded (black) recurrence laws fit to the synthetics. Vertical dashed
 629 lines represent the completeness values.

630

631 From Eq. 9, the annual rates of loss exceedance derived from Fig. 12 are given in
 632 Fig. 13, considering the weak-to-moderate earthquake (M between 5.5 and 7.0). We
 633 assume that event frequency is independent from the date of the most recent
 634 earthquake, for which the Poisson model is used. Unlike Holzer and Savage (2013),
 635 who use a non-stationary Poisson model for losses to take into account the
 636 worldwide population growth, herein, the variables are expressed according to
 637 exposure (exposed population and exposed GDP), i.e., assuming a rate independent
 638 of global population growth. The probability P of observing at least a given loss value

639 in a period of time t is given by:

$$640 \quad P = 1 - e^{-\lambda \Delta t} \quad (10)$$

641 The annual rate of losses over the period 1967-2018 is shown in Figure 13 for
642 F/Pop_{exp} , J/Pop_{exp} and $L\$/GDP_{exp}$.

643

644 For example, from Figure 13 and Eq. 10, the global annual probabilities we obtain
645 are:

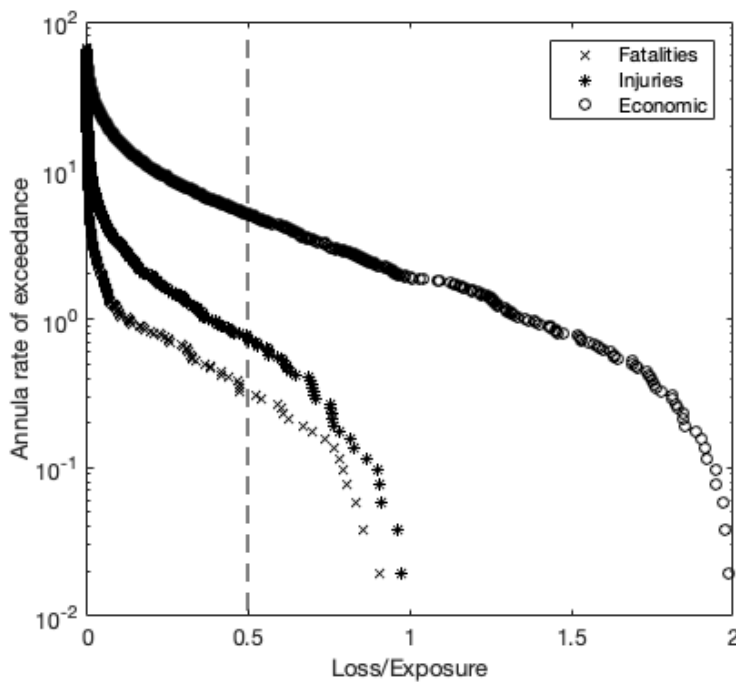
646 $P=0.27$ for $F/Pop_{exp}=0.5$ i.e., 50% of the exposed population has a probability
647 of 27% to die each year;

648 $P=0.50$ for $J/Pop_{exp}=0.5$ i.e., 50% of the exposed population has a probability
649 of 50% to be injured each year;

650 $P=0.99$ for $L\$/GDP_{exp}=0.5$ i.e., 50% of the exposed GDP has a probability of
651 99% to be affected each year.

652

653



654

655 **Figure 13.** Annual rate of exceedance for social and economic losses, considering
656 magnitude $[5.5;7.0[$ earthquakes over the period 1967-2018. Dashed line

657 corresponds to 50% of exposure.

658

659 These results should be taken with caution, as the uncertainties (and their effects)
660 estimated at each stage of the generation of the synthetic loss database have an
661 important impact on the final assessment. Once each earthquake has been defined,
662 intensities are estimated to estimate the level of shaking and its spatial distribution.
663 The spatial cross-correlation of the aleatory (random) variability in the ground motion
664 model should ideally be accounted for, by repeating the scenario event many times,
665 and producing hundreds of possible simulation of the ground motion over the area of
666 interest, and then hundreds of possible losses. Same repeating simulation should be
667 done for each input parameters of the databases and the at each step of the model
668 developed herein. The mean and standard deviation of the loss for the whole
669 exposure model could then be estimated. Nevertheless, this first attempt to build a
670 synthetic seismic losses catalogue as complete as possible at a global scale allows
671 giving a level of risk, in particular for weak-to-moderate earthquakes which remain
672 the least documented events over the period concerned, even though they contribute
673 (in cumulative terms) significantly.

674

675

676 **6. Conclusions**

677

678 In this study, data for 7,515 global seismic events were collected to create a synthetic
679 database of losses associated with earthquakes since 1967 with magnitudes
680 between 5.5 and 8, macroseismic intensities above IV, and affecting populations. At
681 each step of the process, prediction models were developed using data for which all
682 the variables were available (concerning the hazard event, exposure and losses) and
683 tested by the LH method (Scherbaum et al., 2004).

684

685 Like Dollet and Guéguen (2022), we observed that the strongest ($M \geq 7$) (low
686 probabilities-high-consequences) earthquakes make a significant contribution to
687 economic losses (64%), and social losses (44% fatalities and 29% people injured).
688 However, weak-to-moderate earthquakes [5.5; 6.9] also make a sizeable
689 contribution. Compared with high magnitude earthquakes ($M \geq 7$), the lesser

690 consequences of these more frequent earthquakes add up to represent a large
691 proportion of social losses (56% of all deaths and 71% of people injured), while the
692 strongest earthquakes make the largest contribution to economic losses (64% of all
693 economic losses). Efforts must be continued to increase the number of post-seismic
694 reports concerning events of moderate magnitude that cause losses and describe
695 parameters related to the hazard event itself, its consequences, and exposure, and
696 detailing more the direct/indirect losses ratio or even cascading effect that may
697 spread outside directly exposed areas.

698

699 To calculate the losses, variables related to exposure for each macroseismic
700 intensity produce models with better estimations (less uncertainty). This might be
701 further improved if the post-seismic observations of economic and social losses were
702 recorded by macroseismic intensity and not just overall. The models could also be
703 improved by taking into account variables concerning the seismic vulnerability of
704 buildings, which were not considered in this study. These exposure parameters
705 demand a detailed analysis of the zone considered to assess the vulnerability of both
706 assets and people.

707 Finally, economic and social loss occurrence models have been produced to enable
708 the estimation of the probability of fatalities and injuries compared with the exposed
709 population and economic losses compared with the exposed GDP. This loss
710 assessment method provides a stationary distribution of the earthquakes causing
711 losses, assuming a homogeneous distribution of exposures per intensity and over
712 time.

713

714 With the uncertainty values being evaluated at each step of the process, it will be
715 possible to estimate the errors and test the sensitivity of the results at each step. This
716 missing issue is not considered in this study and must be analyzed separately.

717

718 **7. Funding**

719 This work was supported by the Fondation MAIF (URBASIS-Décision: Analyse multi-
720 critères de la réglementation parasismique applicable aux bâtiments publics.
721 Responsabilité acceptable), the European Union's H2020 research and innovation
722 programme under the Maria Skłodowska-Curie (URBASIS-EU, grant agreement N°

723 813137) and funding from Labex OSUG@2020 (Investissements d'avenir, ANR10-
724 LABX56).

725 **8. Competing interests**

726 The authors have no relevant financial or non-financial interests to disclose.

727

728 **9. Author contributions**

729 Philippe Guéguen contributed to the study conception and design, analysis of the
730 data and results and commented on previous versions of the manuscript. Material
731 preparation, data collection and analysis were performed by Cyrielle Dollet. The first
732 draft of the manuscript was written by Cyrielle Dollet. Andres Hernandez contributed
733 to the occurrence model section 7. All authors commented on previous versions of
734 the manuscript. All authors read and approved the final manuscript.

735

736

737

738

739 **10. References**

740

741 Allen, T. I., Wald, D. J., Earle, P. S., Marano, K. D., Hotovec, A. J., Lin, K., & Hearne,
742 M. G. (2009). An Atlas of ShakeMaps and population exposure catalog for
743 earthquake loss modeling. *Bulletin of Earthquake Engineering*, 7(3), 701-718.

744

745 Atkinson, G. M., & Wald, D. J. (2007). "Did You Feel It?" intensity data: A surprisingly
746 good measure of earthquake ground motion. *Seismological Research Letters*, 78(3),
747 362-368.

748

749 Badal, J., & Samardzhieva, E. (2002). Prognostic estimations of casualties caused by
750 strong seismic impacts. *Bulletin of the Seismological Society of America*, 92(6),
751 2310-2322.

752

753 Badal, J., Vázquez-Prada, M., & González, Á. (2005). Preliminary quantitative
754 assessment of earthquake casualties and damages. *Natural Hazards*, 34(3), 353-
755 374.

756

757 Bakun, W. H., & Scotti, O. (2006). Regional intensity attenuation models for France
758 and the estimation of magnitude and location of historical earthquakes. *Geophysical*
759 *Journal International*, 164(3), 596-610.

760

761 Bindi, D., Parolai, S., Oth, A., Abdrakhmatov, K., Muraliev, A., & Zschau, J. (2011).
762 Intensity prediction equations for Central Asia. *Geophysical Journal International*,
763 187(1), 327-337.

764

765 Cha, L. S. (1998). Assessment of global seismic loss based on macroeconomic
766 indicators. *Natural Hazards*, 17(3), 269-283.

767

768 Christoskov, L., & Samardjieva, E. (1984). An approach for estimation of the possible
769 number of casualties during strong earthquakes. *Bulg Geophys J*, 4, 94-106.

770

771 Coburn, A., & Spence, R. (2003). *Earthquake protection*. John Wiley & Sons.

772

773 Daniell, J.E., Schaefer, A.M., & Wenzel, F. (2017). Losses Associated with
774 Secondary Effects in Earthquakes. *Front. Built Environ.*
775 <https://doi.org/10.3389/fbuil.2017.00030>

776

777 Desinventar (2018) Sendai Framework for disaster risk reduction database.
778 <http://www.desinventar.net/DesInventar/results.jsp>. Last access: June 2018

779

780 Di Giacomo, D., Engdahl, E. R., & Storchak, D. A. (2018). The ISC-GEM earthquake
781 catalogue (1904–2014): status after the extension project. *Earth System Science*
782 *Data*, 10(4), 1877-1899.

783

784 Dollet, C., & Guéguen, P. (2022). Global occurrence models for human and
785 economic losses due to earthquakes (1967–2018) considering exposed GDP and
786 population. *Natural Hazards*, 110(1), 349-372.

787

788 Douglas, J. (2003). Earthquake ground motion estimation using strong-motion
789 records: a review of equations for the estimation of peak ground acceleration and
790 response spectral ordinates. *Earth-Science Reviews*, 61(1-2), 43-104.

791

792 EM-DAT (2022) EM-DAT: International disaster database. Université Catholique de
793 Louvain, Belgium. <http://www.emdat.be>. Last Access : June 2018

794

795 Eurostat (2018). <https://ec.europa.eu/eurostat/fr/data/browse-statistics-by-theme>.
796 Last Access: June 2018

797

798 Guettiche, A., Guéguen, P., & Mimoune, M. (2017). Economic and human loss
799 empirical models for earthquakes in the mediterranean region, with particular focus
800 on Algeria. *International Journal of Disaster Risk Science*, 8(4), 415-434.

801

802 Heatwole, N., & Rose, A. (2013). A reduced-form rapid economic consequence
803 estimating model: Application to property damage from US earthquakes. *International*
804 *Journal of Disaster Risk Science*, 4(1), 20-32.

805
806 Holzer, T. L., & Savage, J. C. (2013). Global earthquake fatalities and population.
807 *Earthquake Spectra*, 29(1), 155-175.
808
809 ISC-GEM Global Instrumental Earthquake Catalogue (2019) - Version 6.0, 7 March
810 2019 - <http://doi.org/10.31905/D808B825>
811
812 Jaiswal, K., & Wald, D. (2010). An empirical model for global earthquake fatality
813 estimation. *Earthquake Spectra*, 26(4), 1017-1037.
814
815 Jaiswal, K., & Wald, D. J. (2013). Estimating economic losses from earthquakes
816 using an empirical approach. *Earthquake Spectra*, 29(1), 309-324.
817
818 Levret, A., Backe, J. C., & Cushing, M. (1994). Atlas of macroseismic maps for
819 French earthquakes with their principal characteristics. *Natural hazards*, 10(1), 19-46.
820
821 Musson, R. M., Grünthal, G., & Stucchi, M. (2010). The comparison of macroseismic
822 intensity scales. *Journal of Seismology*, 14(2), 413-428.
823
824 Nichols, J. M., & Beavers, J. E. (2008). World earthquake fatalities from the past:
825 implications for the present and future. *Natural Hazards Review*, 9(4), 179.
826
827 Nievas, C. I., Bommer, J. J., Crowley, H., & van Elk, J. (2020a). Global occurrence
828 and impact of small-to-medium magnitude earthquakes: a statistical analysis. *Bulletin*
829 *of Earthquake Engineering*, 18(1), 1-35.
830
831 Nievas, C. I., Bommer, J. J., Crowley, H., van Elk, J., Ntinalexis, M., & Sangirardi, M.
832 (2020b). A database of damaging small-to-medium magnitude earthquakes. *Journal*
833 *of Seismology*, 24(2), 263-292.
834
835 National Geophysical Data Center / World Data Service (NGDC/WDS): NCEI/WDS
836 Global Significant Earthquake Database. NOAA National Centers for Environmental
837 Information. doi:10.7289/V5TD9V7K [Last access : June 2022]
838
839 Ogata, Y., & Katsura, K. (1993). Analysis of temporal and spatial heterogeneity of
840 magnitude frequency distribution inferred from earthquake catalogues. *Geophysical*
841 *Journal International*, 113(3), 727-738.
842
843 Riedel, I., Gueguen, P., Dunand, F., & Cottaz, S. (2014). Macroscale vulnerability
844 assessment of cities using association rule learning. *Seismological Research Letters*,
845 85(2), 295-305.
846
847 Riedel, I., Guéguen, P., Dalla Mura, M., Pathier, E., Leduc, T., & Chanussot, J.
848 (2015). Seismic vulnerability assessment of urban environments in moderate-to-low

849 seismic hazard regions using association rule learning and support vector machine
850 methods. *Natural hazards*, 76(2), 1111-1141.

851

852 Scherbaum, F., Cotton, F., & Smit, P. (2004). On the use of response spectral-
853 reference data for the selection and ranking of ground-motion models for seismic-
854 hazard analysis in regions of moderate seismicity: The case of rock motion. *Bulletin*
855 *of the seismological society of America*, 94(6), 2164-2185.

856

857 Spence, R., So, E., Jenkins, S., Coburn, A., & Ruffle, S. (2011a). A global
858 earthquake building damage and casualty database. In *Human Casualties in*
859 *Earthquakes* (pp. 65-79). Springer, Dordrecht.

860

861 Schumacher, I., & Strobl, E. (2011). Economic development and losses due to
862 natural disasters: The role of hazard exposure. *Ecological Economics*, 72, 97-105.

863

864

865 UN (2019) United Nations DESA / Population Division. <https://population.un.org/wpp/>.
866 Last access: Jul 2019

867

868 Wald, D. J., Quitoriano, V., Heaton, T. H., Kanamori, H., Scrivner, C. W., & Worden,
869 C. B. (1999). TriNet "ShakeMaps": Rapid generation of peak ground motion and
870 intensity maps for earthquakes in southern California. *Earthquake Spectra*, 15(3),
871 537-555.

872

873 World Bank (2019) The World Bank IBRD/IDA.
874 <https://data.worldbank.org/indicator/sp.pop.totl>. Last access: Jul 2019

875

876 Wyss, M., & Trendafiloski, G. (2011). Trends in the casualty ratio of injured to
877 fatalities in earthquakes. In *Human casualties in earthquakes* (pp. 267-274).
878 Springer, Dordrecht.

879

880

881

882